Optical absorption properties of laser-driven matter

Bing Gu[1] and Ignacio Franco[1,2,*]
[1]*Department of Chemistry, University of Rochester, Rochester, New York 14627, USA*
[2]*Department of Physics, University of Rochester, Rochester, New York 14627, USA*

(Received 21 June 2018; published 12 December 2018)

Characterizing and controlling matter driven far from equilibrium represents a major challenge for science and technology. Here, we develop a theory for the optical absorption of electronic materials driven far from equilibrium by resonant and nonresonant lasers. In it, the interaction between matter and the driving light is treated exactly through a Floquet analysis, while the effects of the probing light are captured to first order in perturbation theory. The resulting equations are reminiscent to those for equilibrium absorption but with the Floquet modes playing the role of the pristine eigenstates. The formalism is employed to characterize the optical properties of a model nanoscale semiconductor dressed by nonresonant light of intermediate intensity (nonperturbative, but nonionizing). As shown, nonresonant light can reversibly turn this transparent semiconductor into a broadband absorber and open strong absorption and stimulated emission bands at very low frequencies (∼meV). Further, the absorption spectra of the driven material exhibit periodic features energetically spaced by the photon energy of the driving light that reflect the periodic structure of the Floquet bands. These developments offer a platform to understand and predict the emergent optical properties of materials dressed by the electric field of light, and catalyze the design of laser-driven materials with desired optical properties.

DOI: 10.1103/PhysRevA.98.063412

I. INTRODUCTION

In the past century we have made remarkable progress in our ability to design, synthesize, and model novel materials with specific functionalities. Many of the insights and tools that we have developed operate at or near equilibrium where the materials are at the minimum of an appropriate thermodynamic potential. Much less is known, however, about the properties and governing principles of matter driven far from equilibrium [1]. In this regime, the effective properties of matter depend on the applied external stimulus and the material response to it. This nonlinear dependency can lead to emergent properties and phenomena that are qualitatively different from those observed near equilibrium (see, e.g., Refs. [2–11]).

Here, we are concerned with the emergent electronic properties of matter driven far from equilibrium by light, in particular, with the ability of these laser-driven materials to absorb light. We envision a physical situation in which a laser drives matter far from equilibrium, while a second perturbative laser source probes its effective ability to absorb light across the electromagnetic spectrum. To capture and interpret the optical properties of laser-driven materials, here we introduce a generalization of the usual theory of linear optical absorption to this nonequilibrium situation where matter is constantly driven by light. New theoretical tools are needed because, in this regime, there is no stationary reference state and energy is no longer a conserved quantity. Thus, the increase of energy of a system from a given reference state can no longer be used as a criterion for the absorption of photons. In addition, the fluctuation-dissipation theorem [12] and Green-Kubo relations [13,14], that form the basis of the usual theory of linear optical absorption [15,16] because they summarize the response of a system near equilibrium to an external weak perturbation, are no longer valid since the Hamiltonian of driven matter is not time-translational invariant. In turn, fully perturbative approaches [16] of the response of matter to both driving and probing pulse, while possible, cannot capture the dynamics induced by the driving pulse exactly in all regimes of the laser-matter interaction.

The theory proposed below overcomes these issues by redefining the absorption properties of driven matter as the rate of transitions induced by the probe photons among the laser-driven states of the system. From this definition, the optical absorption can be expressed by a nonequilibrium dipole-dipole time-correlation function within first-order perturbation theory in the probing light. In turn, the effects of the driving pulse are captured exactly by introducing a Floquet picture into the analysis and focusing on noninteracting electronic materials for which the equations of motion of the fermionic creation and annihilation operators can be closed exactly. The formalism takes into account the quantum statistics of the pristine material, and the nonequilibrium nature of the laser-driven matter, and generalizes previous attempts to define the optical properties of laser-driven matter in various limits [8–10,17–19]. Further, it provides a useful starting point for future efforts to capture additional features introduced by electron-electron, electron-nuclear, or other many-body interactions that can contribute to heating and broadening of the spectral features.

The resulting theory has a structure that is akin to the usual linear absorption theory. However, the photoinduced transitions and transition dipoles that are encountered are

*ignacio.franco@rochester.edu

between single-particle Floquet eigenstates and not between the pristine eigenstates of the system. To demonstrate its utility, we first apply it to a three-level system under resonant driving. As shown, the formalism naturally recovers the well-known Autler-Townes effect [10,20] in which a spectral line in the absorption spectrum splits due to near-resonance laser driving.

Importantly, the theory also provides the technical means to develop physical insights into the absorption properties of driven matter and establish structure-function relations that apply far from equilibrium. In fact, below we use it to explore and interpret the optical properties of a model nanoscale semiconductor dressed by nonresonant lasers. Through Stark effects, nonresonant lasers of intermediate intensity (nonperturbative, but nonionizing) can strongly modify, in a reversible fashion, the electronic structure of extended and nanoscale materials [21–24]. As shown below, in addition to exhibiting a red-shift in the absorption features reminiscent of the Franz-Keldysh effect [25] and the quantum confined Stark effect [26], these laser-driven materials have transient optical properties that are very different from those observed near equilibrium. In fact, we find that nonresonant light can reversibly turn a transparent semiconductor into a broadband absorber and open strong absorption and stimulated emission bands at very low frequencies (∼meV).

The structure of this paper is as follows. In Sec. II, we introduce the optical absorption theory for laser-driven matter. The theory relates the absorption properties to the nonequilibrium two-time dipole-dipole correlation function in the interaction picture of the laser-driven Hamiltonian. Such correlation function is made computationally tractable by adopting a Floquet strategy. In Sec. III, the theory is applied to simulate the nonequilibrium absorption spectrum of a three-level system under resonant driving and a model nanoscale semiconductor under nonresonant driving. The simulated nonequilibrium absorption spectra are interpreted in terms of inter- and intra-Floquet Brillouin zone transitions between Floquet modes. In Sec. IV we summarize our main findings and introduce a qualitative picture for the interpretation of nonequilibrium absorption.

II. THEORY

A. Hamiltonian

We consider the optical properties of a material with Hamiltonian H_M that is constantly being driven by light. The effective Hamiltonian of this laser-driven system is

$$H_{\mathrm{LD}}(t) = H_M + H_d(t), \tag{1}$$

where $H_d(t) = -\boldsymbol{\mu}\cdot\mathbf{E}_d(t)$ is the laser-matter interaction in dipole approximation, $\mathbf{E}_d(t)$ the electric field of the driving light, and $\boldsymbol{\mu}$ the dipole vector operator. Here and throughout, boldface denotes vector quantities. The driving laser can be of arbitrary strength and shape, and taken to have periodicity T (angular frequency $\Omega = 2\pi/T$) such that $H_d(t+T) = H_d(t)$. For pulsed excitation sources, this treatment is appropriate when the envelope of the driving light changes slowly compared to T. The optical properties of this laser-driven material are probed by allowing the material to interact with a weak perturbative probe laser $\mathbf{E}_p(t)$. The total Hamiltonian of the system interacting with both the drive and probe laser is

$$H(t) = H_{\mathrm{LD}}(t) + H_p(t), \tag{2}$$

where $H_p = -\boldsymbol{\mu}\cdot\mathbf{E}_p(t)$. Because the material is driven out of equilibrium by the driving laser, the equilibrium theory [27] connecting the absorption property and the dipole-dipole correlation function cannot be used here. In the following, we generalize the definition of absorption spectrum to materials driven far from equilibrium.

We adopt the following notation: $\alpha, \beta, \gamma, \delta$ will label single-particle eigenstates of the material Hamiltonian; λ, η Floquet states; n Fourier components; and $|i\rangle, |f\rangle$ many-electron states.

B. Optical response of nonequilibrium matter

For definitiveness, we focus on a system that is prepared at time t_0 in a particular many-electron state $|i\rangle$ (with density matrix $\rho = |i\rangle\langle i|$). However, the results presented below are general and apply to initial thermal states, and other nonpure states. To define the optical absorption for nonequilibrium matter, we quantify its response to interaction with a monochromatic probe light at a given frequency ω. Contrary to the equilibrium case, changes in the energy of the system are not a good measure of absorption of light since the energy of the laser-driven system is not conserved [28]. The absorption and stimulated emission can be determined by capturing all physical processes that lead to a change of state of the laser-driven material via interaction with a photon from the probe laser. The rate at which this happens is given by [17,18]

$$I(\omega) = \lim_{t\to\infty} \frac{P(t,\omega)}{t - t_0}, \tag{3}$$

where $P(t,\omega)$ is the probability of a probe photon of frequency ω to lead to change in the laser-driven material after an interaction time interval $t - t_0$.

In this analysis, it is useful to decompose the total evolution operator $U(t,t_0)$ of the system into a part $U_d(t,t_0) = \mathcal{T}e^{-\frac{i}{\hbar}\int_{t_0}^{t} H_{\mathrm{LD}}(\tau)\,d\tau}$ that is due to the driving pulse only, and contributions to the dynamics $S(t,t_0)$ by the probe light in the presence of the driving pulse, i.e.,

$$U(t,t_0) = \mathcal{T}e^{-(i/\hbar)\int_{t_0}^{t} H(\tau)\,d\tau} = U_d(t,t_0)S(t,t_0), \tag{4}$$

where $\mathcal{T}$ denotes time ordering. To understand the physical processes that contribute to $P(t,\omega)$ we introduce a transition amplitude A_{if} between two many-body states $|i\rangle$ and $|f\rangle$ of the pristine material of the form

$$A_{fi} \equiv \langle f|U_d^{\dagger}(t,t_0)U(t,t_0)|i\rangle = \langle f|S(t,t_0)|i\rangle\,. \tag{5}$$

The quantity A_{fi} can be interpreted in two complementary but equivalent ways. It can seen as the overlap between the state of the system at time t, $U(t,t_0)\,|i\rangle$, under the influence of both probe and drive pulses, onto the laser-driven states $U_d(t,t_0)\,|f\rangle$. Alternatively, it can be seen as the projection onto $|f\rangle$ of an initial state that is propagated in a closed time loop. Such a loop consists of forward propagation from $t_0 \to t$ with both lasers turned on and then backwards from $t \to t_0$ with only the driving pulse. This process is akin to the

Kelydysh contour used in the Schwinger-Keldysh formalism [29] and the Loschmidt echo in the study of quantum chaos [30].

The photon scattering operator [or, equivalently, the evolution operator in the interaction picture of $H_{\rm LD}(t)$] $S(t,t_0)$ satisfies a Schrödinger equation $i\hbar\frac{d}{dt}S(t,t_0) = H_{p,I}(t)S(t,t_0)$ $[S(t_0,t_0)=1]$ and admits a Dyson perturbative expansion. Here, $H_{p,I}(t) \equiv U_d^\dagger(t,t_0)H_p(t)U_d(t,t_0)$ is the probe light-matter interaction in the interaction picture of $H_{\rm LD}(t)$. We consider the effect of $H_p(t)$ to first order in perturbation theory where

$$S(t,t_0) = 1 - (i/\hbar)\int_{t_0}^{t} H_{p,I}(t_1)dt_1, \tag{6}$$

so that

$$A_{fi} = \langle f|S(t,t_0)|i\rangle = \langle f\,|\,1 - \frac{i}{\hbar}\int_{t_0}^{t} H_{p,I}(t_1)dt_1\,|\,i\rangle. \tag{7}$$

There are two different types of processes that contribute to $P(t,\omega) = P^{(1)}(t,\omega) + P^{(2)}(t,\omega)$. Those in which, upon interaction, the probe photon leads to amplitude in laser-driven states $U_d(t,t_0)\,|f\rangle$ different from the laser-driven initial state $U_d(t,t_0)\,|i\rangle$, i.e.,

$$P^{(1)}(t,\omega) = \sum_f |A_{fi}|^2 = \frac{1}{\hbar^2}\sum_f \left|\int_{t_0}^{t} dt_1\,\langle f|H_{p,I}(t_1)|i\rangle\right|^2, \tag{8}$$

where the set $\{|f\rangle\}$ consists of every many-body state of the complete basis that is orthogonal to $|i\rangle$, i.e.,

$$1 - |i\rangle\langle i| = \sum_f |f\rangle\langle f|. \tag{9}$$

A second process that leads to absorption and emission of a probe photon is one in which the probe light interacts with any transient dipole in the laser-driven state $U_d(t,t_0)\,|i\rangle$. In this case, the state of the laser-driven material is not changed but absorption and emission of a probe photon occurs, i.e.,

$$\begin{aligned} P^{(2)}(t,\omega) &= |A_{ii}|^2 \\ &= \left|1 - \frac{i}{\hbar}\int_{t_0}^{t} dt_1\,\langle i|H_{p,I}(t_1)|i\rangle\right|^2 \\ &= 1 + \frac{1}{\hbar^2}\int_{t_0}^{t} dt_1|\,\langle i|H_{p,I}(t_1)|i\rangle\,|^2. \end{aligned} \tag{10}$$

This contribution is akin to the interaction of an electric field with a permanent dipole in matter. In the nonequilibrium case, the dipole can be permanent or be induced by the driving pulse.

Combining the two processes, and taking into account Eq. (9),

$$\begin{aligned} P(t,\omega) &= P^{(1)}(t,\omega) + P^{(2)}(t,\omega) \\ &= \frac{1}{\hbar^2}\iint_{t_0}^{t} dt_1dt_2\,\langle i|H_{p,I}(t_1)H_{p,I}(t_2)|i\rangle + 1. \end{aligned} \tag{11}$$

The contribution of the laser-independent term to $P(t,\omega)$ vanishes when calculating the rate in Eq. (3) and will be dropped from this point on. The transition probability $P(t,\omega)$ includes processes to all orders in the driving electric field $\mathbf{E}_d(t)$ and to first order in perturbation theory in the probe electric field $\mathbf{E}_p(t)$. This is reflected by a quadratic dependence of $P(t,\omega)$ on $\mathbf{E}_p(t)$ in Eq. (11). While additional contributions can arise from second-order perturbation theory in $S(t,t_0)$ that also contribute as $|\mathbf{E}_p(t)|^2$, these contributions vanish in $P(t,\omega)$. Thus, Eq. (11) is consistent up to second order in $\mathbf{E}_p(t)$.

To specify the response, it suffices to consider a monochromatic probe pulse $\mathbf{E}_p(t) = \boldsymbol{\varepsilon}_p\cos(\omega t)$ of frequency ω, amplitude $\varepsilon_p = |\boldsymbol{\varepsilon}_p|$, and polarization $\boldsymbol{\varepsilon}_p/\varepsilon_p$. In this case, $H_p(t) = -\mu\varepsilon_p\cos(\omega t)$, where $\mu = \boldsymbol{\mu}\cdot\boldsymbol{\varepsilon}_p/\varepsilon_p$ is the dipole vector operator projected onto the direction of laser polarization. It then follows that the transition probability can be written in a compact way:

$$\begin{aligned} P(t,\omega) = \frac{\varepsilon_p^2}{2\hbar^2}\iint_{t_0}^{t} dt_1dt_2C_{\mu\mu}(t_2,t_1) \\ \times\ \mathrm{Re}[e^{-i\omega(t_1-t_2)} + e^{-i\omega(t_1+t_2)}]. \end{aligned} \tag{12}$$

Here,

$$C_{AB}(t_2,t_1) \equiv \mathrm{Tr}[\rho A_I(t_2)B_I(t_1)] \tag{13}$$

is a two-time correlation function where $A_I(t)$, $B_I(t)$ are system operators in interaction picture of $H_{\rm LD}(t)$, i.e., $A_I(t) = U_d^\dagger(t,t_0)AU_d(t,t_0)$. The final expression for the rate of absorbing and emitting a photon is given by

$$\begin{aligned} I(\omega) = \lim_{t\to\infty}\frac{|\varepsilon_p|^2}{2\hbar^2}\frac{1}{t-t_0}\iint_{t_0}^{t} dt_1dt_2C_{\mu\mu}(t_2,t_1) \\ \times\ \mathrm{Re}[e^{-i\omega(t_1-t_2)} + e^{-i\omega(t_1+t_2)}]. \end{aligned} \tag{14}$$

When $\mathbf{E}_d(t) = 0$, Eq. (14) reduces to the well-known expression $I_{\rm eq}(\omega) \propto \int C(\tau)e^{-i\omega\tau}d\tau$, where $C(\tau) = \langle\mu_I\cdot\mu_I(\tau)\rangle$ for equilibrium systems due to the time-translational invariance in this case [15].

Equation (14) defines the optical response of matter driven by nonperturbative light. It applies to any material, to pure or mixed initial states with density matrix ρ, and to resonant and nonresonant driving pulses of arbitrary intensity. Nevertheless, numerically these equations are challenging to use directly because they require propagating the many-body state to long times and back for each frequency and for each pair of interaction times t_1 and t_2 with the probe field.

Below we specialize our considerations to fermionic systems, and show how further progress can be made by invoking Floquet theorem and focusing on effective noninteracting systems.

C. Optical absorption for laser-driven electronic materials

We consider electronic materials that can be described as an effective noninteracting Hamiltonian, as that expected from time-dependent density functional theory [31,32]. In this case,

$$H_{\rm LD}(t) = \sum_{\alpha\beta} h_{\alpha\beta}(t)c_\alpha^\dagger c_\beta, \tag{15}$$

where the operator $c_\alpha^\dagger$ (or c_α) creates (or annihilates) a fermion in a given single-particle state $|\alpha\rangle$, and where the time dependence arises from the interaction with the driving laser. To calculate $P(t,\omega)$ [Eq. (12)], note that the integrand in

this quantity is determined by the dipole operator $\mu_I(t) = \sum_{\alpha\beta} \mu_{\alpha\beta} c^\dagger_{\alpha,I}(t) c_{\beta,I}(t)$ in the interaction picture. To incorporate the effect of the driving pulse exactly, it is thus necessary to obtain a closed expression for $c_{\alpha,I}(t)$. The equation of motion for the annihilation operator is

$$i\hbar \frac{dc_{\alpha,I}(t)}{dt} = [c_{\alpha,I}(t), H_{\mathrm{LD},I}(t)]. \tag{16}$$

For noninteracting Hamiltonians [Eq. (15)],

$$i\hbar \frac{dc_{\alpha,I}(t)}{dt} = \sum_\beta h_{\alpha\beta}(t) c_{\beta,I}(t). \tag{17}$$

These equations can be solved in closed form to give

$$c_{\alpha,I}(t) = \sum_\beta [\mathcal{U}(t,t_0)]_{\alpha\beta}\, c_\beta, \tag{18}$$

where $\mathcal{U}(t,t_0) \equiv \mathcal{T} e^{-(i/\hbar)\int_{t_0}^t \mathcal{H}(t')\,dt'}$. Here, $\mathcal{H}$ is the effective Hamiltonian of a single particle in the laser-driven system in first quantization with single-particle matrix elements $h_{\alpha\beta} = \langle\alpha|\mathcal{H}|\beta\rangle$. This simplification allows us to introduce Floquet theory at the single-particle level (see Sec. II C 1). The solution in Eq. (18) can be verified by inserting it into Eq. (17) and taking into account that

$$i\hbar \frac{d}{dt}\mathcal{U}(t,t_0) = \mathcal{H}(t)\mathcal{U}(t,t_0), \quad \mathcal{U}(t_0,t_0) = 1. \tag{19}$$

The problem of determining $c_{\alpha,I}(t)$, and thus $P(t,\omega)$, has now been reduced to the problem of determining the single-particle evolution operator $\mathcal{U}(t,t_0)$. Equations (19) and (18) are solved below using Floquet theory.

1. Floquet theory for the single-particle evolution operator

As the dressed material's Hamiltonian is periodic $H_{\mathrm{LD}}(t) = H_{\mathrm{LD}}(t+T)$ ($T = 2\pi/\Omega$), so is $\mathcal{H}(t) = \mathcal{H}(t+T)$. According to the Floquet theorem [4,33,34], for periodically driven Hamiltonians, there exist solutions, so-called Floquet states, to the Schrödinger equation

$$i\hbar \frac{d}{dt}|\psi_\lambda(t)\rangle = \mathcal{H}(t)\,|\psi_\lambda(t)\rangle \tag{20}$$

of the form

$$|\psi_\lambda(t)\rangle = e^{-i\mathcal{E}_\lambda t/\hbar}\,|\phi_\lambda(t)\rangle\,, \quad |\phi_\lambda(t)\rangle = |\phi_\lambda(t+T)\rangle\,, \tag{21}$$

where the $|\phi_\lambda(t)\rangle$ are the so-called Floquet modes and where the quasienergies $\mathcal{E}_\lambda$ are uniquely defined in the first Floquet Brillouin zone (FBZ) $\{-\hbar\Omega/2 \leqslant \mathcal{E}_\lambda < \hbar\Omega/2\}$. Note that the Floquet states $\{|\psi_\lambda(t)\rangle\}$ are single-particle states rather than many-body states. While there exist also many-body Floquet states, in this context, it is much simpler to work at the single-particle level.

To understand Floquet theorem, consider the eigenstates of the evolution operator from t_0 to $t_0 + T$,

$$\mathcal{U}(T)\,|\varphi_\lambda\rangle = e^{-i\mathcal{E}_\lambda T/\hbar}\,|\varphi_\lambda\rangle\,, \tag{22}$$

with eigenvalues $e^{-i\mathcal{E}_\lambda T/\hbar}$, where the energies $\mathcal{E}_\lambda$ are defined by the eigenvalue equation. In this section, for simplicity, we take $t_0 = 0$ and abbreviate $\mathcal{U}(t) \equiv \mathcal{U}(t,t_0)$. The Floquet states of the form in Eq. (21) can be defined as

$$|\psi_\lambda(t)\rangle \equiv \mathcal{U}(t)\,|\varphi_\lambda\rangle = e^{-i\mathcal{E}_\lambda t/\hbar}\,|\phi_\lambda(t)\rangle\,, \tag{23}$$

where we have defined the Floquet mode

$$|\phi_\lambda(t)\rangle = e^{i\mathcal{E}_\lambda t/\hbar}\mathcal{U}(t)\,|\varphi_\lambda\rangle\,. \tag{24}$$

To prove Floquet theorem, it suffices to show the Floquet mode satisfies $|\phi_\lambda(t+T)\rangle = |\phi_\lambda(t)\rangle$. This follows because

$$\begin{aligned} |\phi_\lambda(t+T)\rangle &= e^{i\mathcal{E}_\lambda t/\hbar} e^{i\mathcal{E}_\lambda T/\hbar}\mathcal{U}(t+T,T)\mathcal{U}(T)\,|\varphi_\lambda\rangle \\ &= e^{i\mathcal{E}_\lambda t/\hbar}\mathcal{U}(t+T,T)\,|\varphi_\lambda\rangle \\ &= e^{i\mathcal{E}_\lambda t/\hbar}\mathcal{U}(t)\,|\varphi_\lambda\rangle = |\phi_\lambda(t)\rangle\,, \end{aligned} \tag{25}$$

where we have used the eigenvalue relation (22). All quasienergies $\mathcal{E}_\lambda + n\hbar\Omega$ where n is an integer satisfy the same eigenvalue equation (22) and define the same state. Inserting Eq. (21) into the time-dependent Schrödinger equation yields

$$\left(\mathcal{H}(t) - i\hbar\frac{d}{dt}\right)|\phi_\lambda(t)\rangle = \mathcal{E}_\lambda\,|\phi_\lambda(t)\rangle\,, \tag{26}$$

where $\mathcal{H}(t) - i\hbar\frac{d}{dt}$ is the Floquet Hamiltonian defined in the extended space (Hilbert space $\otimes$ time). For single-particle Hamiltonians, Eq. (26) defines the single-particle Floquet modes and their quasienergies.

Since the Floquet modes are periodic function in time, in addition to their usual expansion in a complete single-particle basis in Hilbert space, they can also be expanded into Fourier components $\{e^{in\Omega t},\ n \in \mathbb{Z}\}$, i.e.,

$$|\phi_\lambda(t)\rangle = \sum_{n,\beta} F^{(\lambda)}_{n\beta} e^{in\Omega t}\,|\beta\rangle\,. \tag{27}$$

Substituting this expansion into Eq. (26), left multiplying by $\langle\alpha|\,e^{-im\Omega t}$ and averaging over a time period $\frac{1}{T}\int_0^T dt$ (i.e., taking the inner product in the extended space) gives the eigenvalue equation

$$\sum_{m,\beta} \Gamma_{n\alpha;m\beta} F^{(\lambda)}_{m\beta} = \mathcal{E}_\lambda \sum_{m,\beta} F^{(\lambda)}_{m\beta}. \tag{28}$$

Here, the matrix elements of the Floquet Hamiltonian are given by

$$\Gamma_{n\alpha;m\beta} = h^{(n-m)}_{\alpha\beta} + n\hbar\Omega\delta_{nm}\delta_{\alpha\beta}, \tag{29}$$

where $\mathcal{H}^{(n)}$ ($h^{(n)}_{\alpha\beta} \equiv \langle\alpha|\mathcal{H}^{(n)}|\beta\rangle$) is the nth Fourier component of the single-particle Hamiltonian of the laser-driven system:

$$\mathcal{H}^{(n)} \equiv \frac{1}{T}\int_0^T dt\, e^{-in\Omega t}\mathcal{H}(t). \tag{30}$$

Equation (28) is a generalized eigenvalue problem defined in a composite basis $\{|\alpha n\rangle \equiv |\alpha\rangle \otimes e^{in\Omega t}\|\alpha \in [1,N],\ n \in \mathbb{Z}\}$, where $|\alpha\rangle$ is any complete basis of the Hilbert space. It can be solved to determine the Floquet states and energies.

Once the Floquet modes $\{|\phi_\lambda(t)\rangle\}$ are determined [Eq. (27)] so will be the propagator $\mathcal{U}(t,t_0)$:

$$\mathcal{U}(t,t_0) = \sum_\lambda e^{-i\mathcal{E}_\lambda(t-t_0)/\hbar}\,|\phi_\lambda(t)\rangle\,\langle\phi_\lambda(t_0)|\,, \tag{31}$$

where we have made the initial time dependence explicit. Equation (31) satisfies the Schrödinger equation in Eq. (19), as required. Substituting the above into Eq. (18) leads to the

solution for $c_{\alpha,I}(t)$:

$$c_{\alpha,I}(t) = \sum_{\lambda} e^{-i\mathcal{E}_\lambda(t-t_0)/\hbar} \sum_{n\beta} F^{(\lambda)}_{n\alpha} e^{in\Omega t} \langle \phi_\lambda(t_0)|\beta\rangle\, c_\beta. \quad (32)$$

Equations (31) and (32) can now be used to compute correlation functions and the spectrum as described below.

2. Correlation function in Floquet theory

To calculate the two-time dipole-dipole correlation function [Eq. (13)], the dipole operator in the interaction picture of $H_{\rm LD}(t)$ is required. Inserting Eq. (18) into $\mu_I(t) = \sum_{\alpha\beta} \mu_{\alpha\beta} c^\dagger_{\alpha,I}(t) c_{\beta,I}(t)$, where $\mu_{\alpha\beta} = \langle\alpha|\tilde{\mu}|\beta\rangle$ and $\tilde{\mu}$ is the single-particle dipole operator, yields

$$\begin{aligned}\mu_I(t) &= \sum_{\alpha,\beta,\gamma,\delta} \mu_{\alpha\beta} [\mathcal{U}^\dagger(t,t_0)]_{\gamma\alpha} c^\dagger_\gamma [\mathcal{U}(t,t_0)]_{\beta\delta}\, c_\delta \\ &= \sum_{\gamma,\delta} \langle\gamma\,|\,\mathcal{U}^\dagger(t,t_0)\tilde{\mu}\mathcal{U}(t,t_0)\,|\,\delta\rangle c^\dagger_\gamma c_\delta \\ &= \sum_{\lambda'\lambda}\sum_{\gamma\delta} \mu_{\lambda'\lambda}(t) e^{i\mathcal{E}_{\lambda'\lambda}(t-t_0)/\hbar} \left\langle\gamma\middle|\phi^0_{\lambda'}\right\rangle\left\langle\phi^0_\lambda\middle|\delta\right\rangle c^\dagger_\gamma c_\delta,\end{aligned} \quad (33)$$

where we have used Eq. (31) and the fact that $\sum_\alpha |\alpha\rangle\langle\alpha| = 1$. Here, $\mu_{\lambda'\lambda}(t) = \langle\phi_{\lambda'}(t)|\tilde{\mu}|\phi_\lambda(t)\rangle$ is the time-dependent transition dipole between Floquet modes $|\phi^0_\lambda\rangle \equiv |\phi_\lambda(t_0)\rangle$ and $\mathcal{E}_{\lambda'\lambda} = \mathcal{E}_{\lambda'} - \mathcal{E}_\lambda$.

Because the Floquet modes are periodic, so is the dipole matrix $\mu_{\lambda'\lambda}(t) = \mu_{\lambda'\lambda}(t+T)$ such that it admits a Fourier expansion

$$\mu_{\lambda'\lambda}(t) = \sum_{n=-\infty}^{\infty} \mu^{(n)}_{\lambda'\lambda} e^{in\Omega t} \quad (34)$$

with the expansion coefficients

$$\mu^{(n)}_{\lambda'\lambda}(t) = \frac{1}{T}\int_0^T \mu_{\lambda'\lambda}(t) e^{-in\Omega t}\, dt. \quad (35)$$

Inserting this expansion into Eq. (33) yields

$$\mu_I(t) = \sum_{\lambda',\lambda,\gamma,\delta}\sum_n D^n_{\lambda'\lambda\gamma\delta} e^{i\mathcal{E}_{\lambda'\lambda}(t-t_0)/\hbar + in\Omega t} c^\dagger_\gamma c_\delta, \quad (36)$$

where

$$D^n_{\lambda'\lambda\gamma\delta} = \mu^{(n)}_{\lambda'\lambda}\langle\gamma\,|\,\phi^0_{\lambda'}\rangle\langle\phi^0_\lambda\,|\,\delta\rangle. \quad (37)$$

The correlation function can then be obtained by inserting Eq. (36) into Eq. (13):

$$\begin{aligned}C_{\mu\mu}(\bar{t},\tau) = &\sum_{n,n'}\sum_{\lambda,\lambda',\eta,\eta'}\sum_{\gamma\delta\gamma'\delta'} D^n_{\lambda'\lambda\gamma\delta} \\ &\times D^{n'}_{\eta'\eta\gamma'\delta'} e^{i(\mathcal{E}_{\eta'\eta}+\mathcal{E}_{\lambda'\lambda})(\bar{t}-t_0)/\hbar + i(n'+n)\Omega\bar{t}} \\ &\times e^{i[(\mathcal{E}_{\eta'\eta}-\mathcal{E}_{\lambda'\lambda})/\hbar + (n'-n)\Omega]\tau/2} \langle c^\dagger_\gamma c_\delta c^\dagger_{\gamma'} c_{\delta'}\rangle,\end{aligned} \quad (38)$$

where, for future convenience, we have transformed the two time arguments into a center of mass $\bar{t} = \frac{t_1+t_2}{2}$ and a relative time variable $\tau = t_2 - t_1$. For a system initially prepared in a statistical mixture of single Slater determinants, the term $\langle c^\dagger_\gamma c_\delta c^\dagger_{\gamma'} c_{\delta'}\rangle$ entering into the correlation function [Eq. (38)] can be computed as follows. This term does not vanish in two different cases, $\gamma = \delta$, $\gamma' = \delta'$ and $\gamma = \delta'$, $\delta = \gamma'$, which give

$$\begin{aligned}\Lambda_{\gamma\delta\gamma'\delta'} &\equiv \langle c^\dagger_\gamma c_\delta c^\dagger_{\gamma'} c_{\delta'}\rangle \\ &= \delta_{\gamma\delta}\delta_{\gamma'\delta'}\bar{n}_\gamma\bar{n}_{\gamma'} + \delta_{\gamma'\delta}\delta_{\gamma\delta'}\bar{n}_\gamma(1-\bar{n}_{\gamma'}),\end{aligned} \quad (39)$$

where $n_\gamma \equiv c^\dagger_\gamma c_\gamma$ is the number operator and $\bar{n}_\gamma = \mathrm{Tr}\{\rho n_\gamma\}$ the initial distribution function of the single-particle energy eigenstates. For thermal initial states, $\bar{n}_\gamma$ corresponds to the Fermi-Dirac distribution.

3. Time integration and final expressions

In the center of mass and relative time variables the rate of absorption and emission [Eq. (14)] is given by

$$\begin{aligned}I(\omega) = \lim_{t\to\infty} \frac{\varepsilon_p^2}{2\hbar^2}\frac{1}{t-t_0}\iint_{t_0}^{t} dt_1 dt_2 C_{\mu\mu}(\bar{t},\tau) \\ \times\ \mathrm{Re}[e^{-i\omega\tau} + e^{-i2\omega\bar{t}}].\end{aligned} \quad (40)$$

We take the preparation time of the system to be in the remote past, such that $t_0 \to -\infty$. In this limit, the two-time integral in Eq. (14) reduces to Fourier transforms, i.e.,

$$\begin{aligned}I(\omega) = \lim_{t\to\infty} \frac{\varepsilon_p^2}{2\hbar^2}\frac{1}{t-t_0}\iint_{-\infty}^{t} d\bar{t}\, d\tau\, C_{\mu\mu}(\bar{t},\tau) \\ \times\ \mathrm{Re}[e^{-i\omega\tau} + e^{-i2\omega\bar{t}}].\end{aligned} \quad (41)$$

The second complex exponential term that depends on $\bar{t}$ in Eq. (41) does not contribute to $I(\omega)$ (see Appendix for details). It suffices then to focus on the $e^{-i\omega\tau}$ term, i.e.,

$$I(\omega) = \frac{\varepsilon_p^2}{4\hbar^2}\lim_{t\to+\infty}\frac{1}{t-t_0}\iint_{-\infty}^{t} C_{\mu\mu}(\bar{t},\tau)(e^{-i\omega\tau} + \mathrm{c.c.})\, d\bar{t}\, d\tau. \quad (42)$$

Inserting Eq. (38) into the above equation, one notices that the integration with respect to $\bar{t}$ gives oscillatory contributions whose contribution to $I(\omega)$ vanishes at $t \to +\infty$ except when the oscillatory factor is zero. In that case, the integration leads to a $(t-t_0)$ term that cancels the $1/(t-t_0)$ in the expression for $I(\omega)$. This happens when $\mathcal{E}_{\eta'\eta} + \mathcal{E}_{\lambda'\lambda} = 0$ and $n + n' = 0$. The former condition implies that either $\eta' = \lambda$, $\eta = \lambda'$ or $\eta' = \eta$, $\lambda' = \lambda$. Taking this into account, the absorption spectrum can be written as

$$\begin{aligned}I(\omega) = \frac{\varepsilon_p^2}{4h}\sum_{\gamma\delta\gamma'\delta'}\sum_{\lambda,\lambda'}\sum_n \big[&D^n_{\lambda\lambda\gamma\delta} D^{-n}_{\lambda'\lambda'\gamma'\delta'}\delta(n\hbar\Omega - \hbar\omega) \\ &+ D^{-n}_{\lambda\lambda'\gamma\delta} D^n_{\lambda'\lambda\gamma'\delta'}\delta(\mathcal{E}_{\lambda'\lambda} + n\hbar\Omega - \hbar\omega)\big]\Lambda_{\gamma\delta\gamma'\delta'} \\ &+ (\omega \leftrightarrow -\omega),\end{aligned} \quad (43)$$

where the last term corresponds to the same expression but replacing ω with $-\omega$, and where we have taken into account of the integral representation of the delta function $\delta(\omega) = \frac{1}{2\pi}\int_{-\infty}^{+\infty} e^{i\omega t}\, dt$ and $\delta(\hbar\omega) = \delta(\omega)/\hbar$.

The quantity $I(\omega)$ measures the rate of change induced by the probe photons on the laser-driven material. However, it does not tell us whether the change is due to absorption or stimulated emission processes. We identify the first two terms in Eq. (43) as optical absorption because $\omega > 0$ and the delta

functions in Eq. (43) will only be nonzero when the energy difference between the Floquet states involved $\mathcal{E}_{\lambda'\lambda} + n\hbar\Omega$ is positive, leading to absorption of photons from the probe field. By contrast, the $-\omega$ term corresponds to stimulated emission. The net absorption of probe photons by the laser-driven material would correspond to the difference between these two contributions:

$$A(\omega) = \frac{|\varepsilon_p|^2}{4h} \sum_{\lambda,\lambda'} \sum_{\gamma\gamma'} \sum_{n} \left(D^{-n}_{\lambda\lambda'\gamma\gamma'} D^{n}_{\lambda'\lambda\gamma'\gamma}\right) \times [\delta(\mathcal{E}_{\lambda'\lambda} + n\hbar\Omega - \hbar\omega) - \delta(\mathcal{E}_{\lambda'\lambda} + n\hbar\Omega + \hbar\omega)] \times \bar{n}_\gamma(1 - \bar{n}_{\gamma'}), \tag{44}$$

where we have taken into account that the $\delta(n\hbar\Omega - \hbar\omega)$ and $\bar{n}_\gamma \bar{n}_{\gamma'}$ contribution exactly cancel. Inserting Eq. (37) into Eq. (44) and introducing

$$P_{\lambda\lambda'} \equiv \sum_{\gamma\gamma'} \left|\langle \phi^0_\lambda \mid \gamma\rangle\right|^2 \left|\langle \phi^0_{\lambda'} \mid \gamma'\rangle\right|^2 \bar{n}_\gamma(1 - \bar{n}_{\gamma'}), \tag{45}$$

which acts as an effective population factor between the Floquet modes, yields the final expression of the absorption spectrum for laser-driven matter

$$A(\omega) = \frac{|\varepsilon_p|^2}{4h} \sum_{\lambda,\lambda'} \sum_{n} \left|\mu^{(n)}_{\lambda'\lambda}\right|^2 P_{\lambda\lambda'} [\delta(\mathcal{E}_{\lambda'\lambda} + n\hbar\Omega - \hbar\omega) - \delta(\mathcal{E}_{\lambda'\lambda} + n\hbar\Omega + \hbar\omega)], \tag{46}$$

where we have taken into account that $\mu^{(-n)}_{\lambda\lambda'} = \mu^{(n)*}_{\lambda'\lambda}$.

Equation (46) offers a clear structure for the interpretation of nonequilibrium absorption, that is analogous to the one encountered in equilibrium absorption theory. The Floquet modes play the role of system eigenstates and the effective population factor $P_{\lambda\lambda'}$ characterize the probability that $|\phi_\lambda\rangle$ is occupied while the state $|\phi_{\lambda'}\rangle$ is unoccupied. The first term captures absorption when the frequency of the probing light is at resonance with a transition frequency between two Floquet modes $\mathcal{E}_{\lambda'\lambda} + n\hbar\Omega$. In turn, the second term is stimulated emission. The states must be connected by a nonzero transition dipole $\mu^{(n)}_{\lambda\lambda'}$ for a transition to occur.

An additional feature that arises from the time dependence of Floquet states is that the effective dipole operator $\mu^{(n)}_{\lambda\lambda'}$ has an extra index n, originating from the periodicity of the Floquet states. This extra index can be understood as the indicator for intra- or inter-FBZ transitions. When $n = 0$, it indicates that the transitions are inside the same FBZ. In turn, when $n \neq 0$ the transitions happen between different FBZs and n indicates the number of FBZs that separates the two Floquet states. This transition is analogous to the umklapp process in solids where the crystal momentum is changed into another Brillouin zone as a result of a scattering process. The probability for different number of FBZs to be involved depends on the details of the system, the strength and frequency of the driving laser. Note that while for equilibrium absorption $\mu_{\alpha\beta} = \mu^\star_{\beta\alpha}$, for nonequilibrium absorption, $\mu^{(n)}_{\lambda\lambda'} \neq \mu^{(n)\star}_{\lambda'\lambda}$ except for $n = 0$.

Equation (46) shows that one can naturally interpret nonequilibrium absorption as optical transitions among Floquet states. Aside from atoms, molecules, and nanoscale systems, Eq. (46) can also be applied to solids if the single-particle states are taken as Bloch states. In that case, it is interesting to contrast Eq. (46) to previous efforts to develop theories of laser-driven semiconductors [17,18,35]. Equation (46) generalizes the results in [17,18] by providing a physically transparent derivation of the nonequilibrium optical absorption and clarifying its basic structure, incorporating the effects of quantum statistics and, importantly, by recognizing the role of stimulated emission processes in $P(t, \omega)$.

By adopting a Floquet strategy, we have been able to reduce the dynamic problem of optical absorption and stimulated emission of laser-driven matter to a static problem that requires sums over Floquet states and single-particle energy eigenstates. These states can be obtained via simple diagonalization techniques. To calculate $A(\omega)$, it is necessary to do the following: (i) Diagonalize the material Hamiltonian H_M to obtain the single-particle energy eigenstates $\{|\alpha\rangle\}$ and express the dipole operator in this basis. (ii) Construct the Floquet Hamiltonian matrix (29) and solve Eq. (28) by diagonalization to obtain the quasienergies $\{\mathcal{E}_\lambda\}$ and the expansion coefficients of Floquet modes $\{F_{n\beta}\}$ in the $|\beta n\rangle$ basis. In practice, to solve these equations the Floquet Hamiltonian matrix needs to be truncated. Results need to be checked for convergence on the number of Fourier components. (iii) Calculate the effective dipole using Eq. (35) and population factor following the definition in Eq. (45) and use them to compute the absorption spectrum based on Eq. (46). From a numerical perspective, the second step is most challenging because it involves a diagonalization of the Floquet matrix whose size scales as $O(N_b N_F)$ where N_F is the number of Fourier components and N_b is the number of single-particle orbitals of the system. This matrix grows quickly for realistic systems under nonresonant or strong driving.

III. APPLICATIONS OF THE THEORY AND INTERPRETATION OF THE NONEQUILIBRIUM SPECTRA

Using Eq. (46), we are now in a position to quantify and interpret the optical properties of laser-driven matter. The validity of the theory is demonstrated by using it to recover the well-known Autler-Townes effect of laser-driven few-level systems. The utility of the approach, by using it to explore the optical properties of nanoscale semiconductors driven by nonresonant light. As shown, nonperturbative reversible driving with nonresonant light can significantly distort the absorption spectrum leading to a laser-driven material with spectral features that have no equilibrium counterpart. A qualitative scheme to interpret nonequilibrium absorption in the laser-driven picture is developed and used to assign spectral features in both cases.

A. Resonantly driven three-level system

Autler and Townes [10] showed that an optical transition between two levels in a few-level system can be split into a doublet when one of the two levels involved in the transition is coupled to a third one by a strong resonant light, a phenomenon that is also referred as the dynamic Stark splitting. The Autler-Townes (AT) effect has been observed in the absorption spectra of atoms [10], small molecules [37],

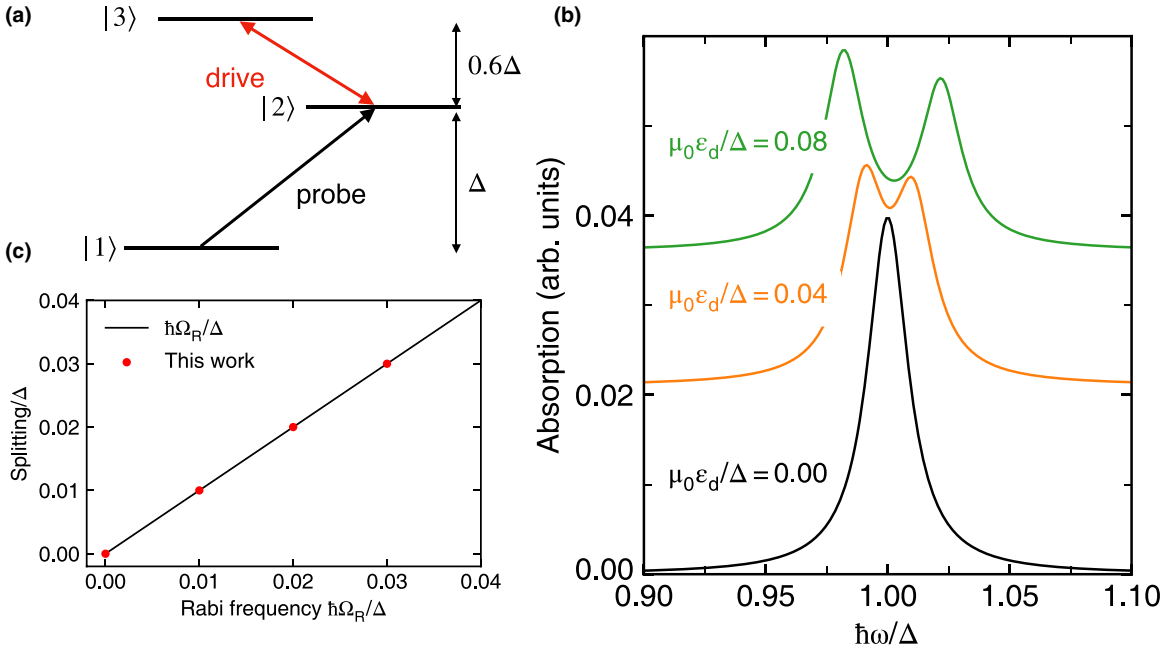

FIG. 1. Simulation of the Autler-Townes splitting using Eq. (46). (a) Energy diagram for a three-level system. The driving pulse resonantly drives the $|2\rangle \rightarrow |3\rangle$ transition, while the probe light measures the optical absorption. Here, $\mu_0 = \langle 1|\,\mu\,|2\rangle = \langle 2|\,\mu\,|3\rangle$ are the nonzero transition dipoles. (b) The absorption spectrum computed using Eq. (46) (broadened with a Lorentzian function of width 0.01Δ) under different driving amplitudes ε_d naturally exhibits the Autler-Townes splitting. (c) The AT splitting yielded by Eq. (46) is $\hbar\Omega_{\rm R}$ where $\Omega_{\rm R} \equiv \mu_0\varepsilon_d/\hbar$ is the Rabi frequency in quantitative agreement with theoretical predictions using a different method [20] and experiments [36].

superconducting Josephson junction [38], and quantum dots [36] dressed by resonant lasers.

To demonstrate that Eq. (46) recovers the AT effect, we computed the nonequilibrium absorption spectra in the three-level system (with states $|1\rangle$, $|2\rangle$, and $|3\rangle$) shown in Fig. 1(a). In the computations, the system is driven by a laser that is resonant with the $|2\rangle \rightarrow |3\rangle$ transition. The resulting absorption spectra is shown in Fig. 1(b). As can be seen, the absorption spectrum clearly exhibits the Autler-Townes splitting, and the slope of the observed linear increase in the splitting with ε_d is in quantitative agreement with previous theoretical and experimental observations [Fig. 1(c)] [36].

The interpretation of the AT effect is a well-developed subject [9,20]. In the laser-dressed picture it can be understood through resonances induced by resonant driving between Floquet states, and their subsequent Rabi splitting. It is instructive to interpret this phenomenon through Eq. (46). For definiteness, consider the $\mu_0\varepsilon_d/\Delta = 0.04$ case. Figure 2(b) shows the quasienergies in the first FBZ and overlap between Floquet modes at times $t_0 + nT$ and the pristine states. As can be seen, the Floquet modes $|\phi_1\rangle$, $|\phi_2\rangle$ are a linear combination of the two pristine states $|2\rangle$ and $|3\rangle$, that are under resonant driving while the Floquet mode $|\phi_3\rangle$ is just the pristine state $|1\rangle$. The two transitions, labeled by X, Y in Fig. 2(a), are transitions between Floquet modes $|\phi_3\rangle \rightarrow |\phi_1\rangle$, $|\phi_2\rangle$ separated by two FBZs, respectively. The corresponding effective transition dipole and population factor for these two transitions are marked in Figs. 2(c) and 2(d). Clearly, these two transitions are allowed by population and transition dipoles. Other intraband and interband transitions with nonzero transition dipoles are not allowed by the population factor.

B. Nonresonantly driven tight-binding nanostructure

We now focus on the optical properties of a generic two-band semiconducting nanostructure driven by nonresonant light of intermediate intensity. Through Stark effects, nonresonant light can dramatically distort the electronic structure of nanostructures and extended systems creating a laser-dressed material with effective electronic properties that can be very different from those observed near equilibrium. Below we clarify the optical properties of such laser-driven materials in the context of a minimal one-dimensional tight-binding model. We focus on the reversible regime of the laser-matter interaction where the net absorption of photons by matter from the nonresonant driving pulse is suppressed.

The tight-binding Hamiltonian of a one-dimensional two-band semiconducting nanoparticle with K unit cells is

$$H_M = \sum_{k=1}^{K}(\epsilon_1 c_{2k-1}^\dagger c_{2k-1} + \epsilon_2 c_{2k}^\dagger c_{2k}) - \sum_{k=1}^{K} t_\alpha (c_{2k-1}^\dagger c_{2k} + \text{H.c.}) - \sum_{k=1}^{K-1} t_\beta (c_{2k}^\dagger c_{2k+1} + \text{H.c.}), \tag{47}$$

where $c_k^\dagger$ creates a fermion on site k ($|k\rangle = c_k^\dagger|0\rangle$, where $|0\rangle$ is the vacuum state), and where H.c. stands for Hermitian conjugate. Each unit cell consists of two sites with onsite energies ϵ_1 and ϵ_2 ($\epsilon_1 = -\epsilon_2 = 1.6$ eV) in nearest-neighbor coupling with intracell hopping parameter $t_\alpha = 0.7$ eV and intercell $t_\beta = 1.0$ eV. The lattice constant is taken to be $a = 3.2$ Å and the two sites in each cell to be separated by a distance $b = 0.0$ Å

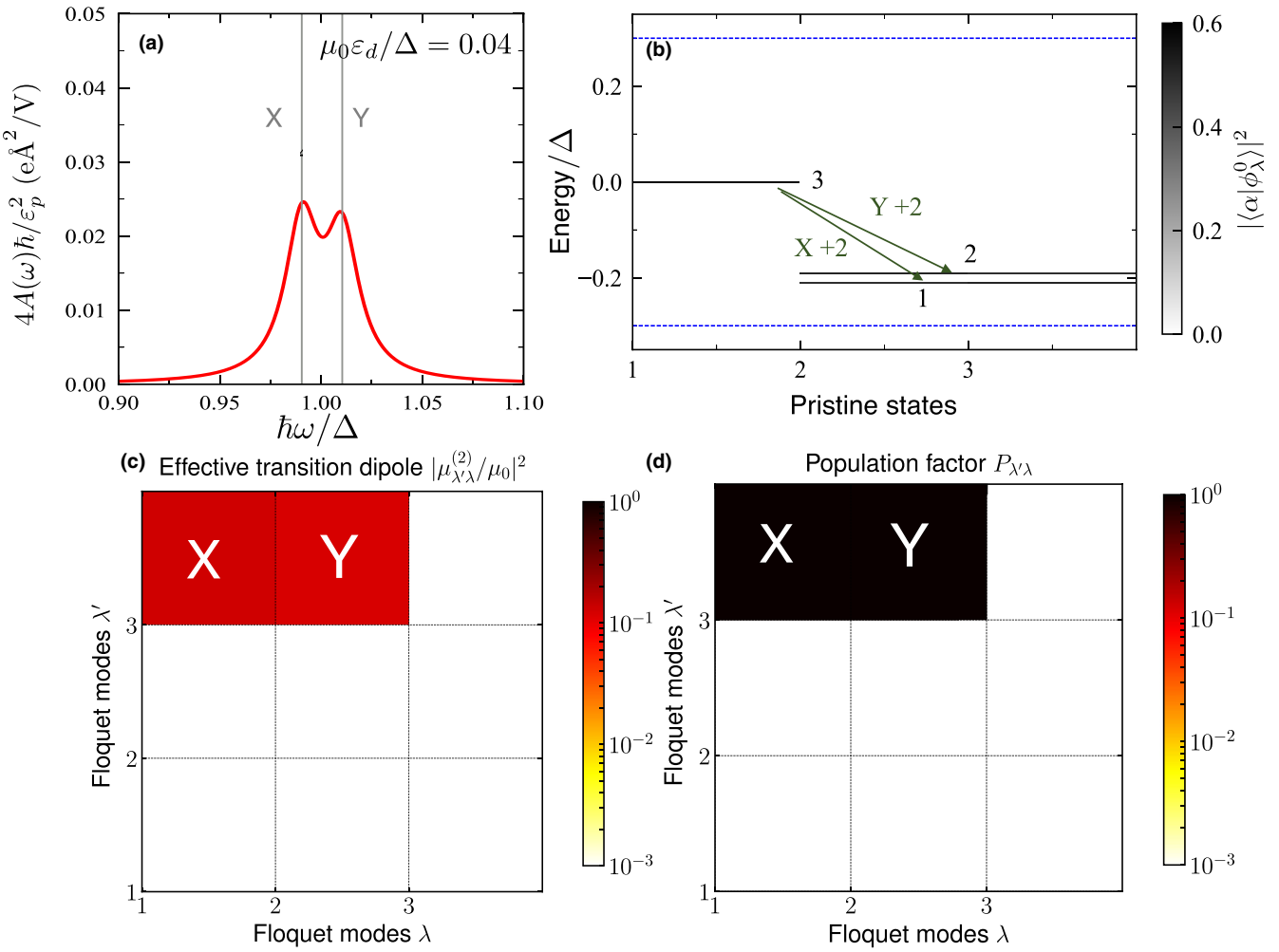

FIG. 2. Interpretation of the nonequilibrium absorption spectra using Eq. (46) of the three-level system in Fig. 1 initially prepared in $|1\rangle$ dressed by light resonant with the $|2\rangle \to |3\rangle$ transition with $\mu_0\varepsilon_d/\Delta = 0.04$. (a) The absorption spectrum has two main transitions labeled X and Y. (b) Overlap between the Floquet modes at times $t_0 + nT$ and the pristine states $|\langle\alpha|\phi_\lambda(t_0)\rangle|^2$ in the first FBZ. The Floquet modes are ordered by the quasienergy in the first FBZ. The optical transitions X and Y are indicated by green arrows with the number of FBZs that separates them $+n$. (c) Effective dipole between Floquet modes two FBZs away. Other nonzero transition dipoles are not allowed by the population factor. (d) Effective population factor $P_{\lambda'\lambda}$ ($\lambda' \to \lambda$) between Floquet modes. The elements in (c) and (d) corresponding to the X, Y transitions are marked.

(i.e., two sites at the same location). These parameters are chosen to resemble the electronic structure of ZnO.

The nanostructure is dressed in dipole approximation by a nonresonant monochromatic laser field with electric field amplitude $E_d(t) = \varepsilon_d \cos(\Omega t)$, and probed with a laser of amplitude $E_p(t) = \varepsilon_p \cos(\omega t)$. Both probe and drive are taken to have their polarization along the length of the nanostructure. At initial time t_0 the system is chosen to be in the ground zero-temperature state. While large system sizes can in principle be considered, below we focus on the $K = 6$ case such that a detailed analysis of all transitions visible in the absorption spectrum is tractable.

We focus on the regime where the frequency of the driving field is much smaller than the band gap $\hbar\Omega = 0.38$ eV $\ll E_g = 3.31$ eV such that Stark effects and not near-resonance multiphoton absorption effects dominate the dynamics. In this regime, the laser-matter interaction is reversible in the sense that, for pulsed driving, after the driving pulse is turned off the system will return to its initial unexcited state. We verify that we are in this regime by explicitly solving the time-dependent Schrödinger equation for the nanostructure under the influence of 200-fs Gaussian pulses with the maximum field amplitude and frequency of E_d, and ensuring that after the pulse there is no net excitation of the chain.

Figure 3 shows the nonequilibrium absorption spectrum of the nanoparticle dressed by lasers of varying amplitude $\varepsilon_d \in [0, 0.4\ \text{V/Å}]$. Blue lines refer to stimulated emission, red lines to net absorption, and the gray lines signal the absorption peaks. Convergence of the absorption spectra requires considering $N_F = 61$ Fourier components symmetrically around $n = 0$. At equilibrium ($\varepsilon_d = 0.00$), the nanoparticle is transparent in the 0–3.2 eV range. Optical transitions start to appear when the frequency of the probing pulse is larger than the band gap. The absorption spectra completely change as the system is driven far from equilibrium even when the

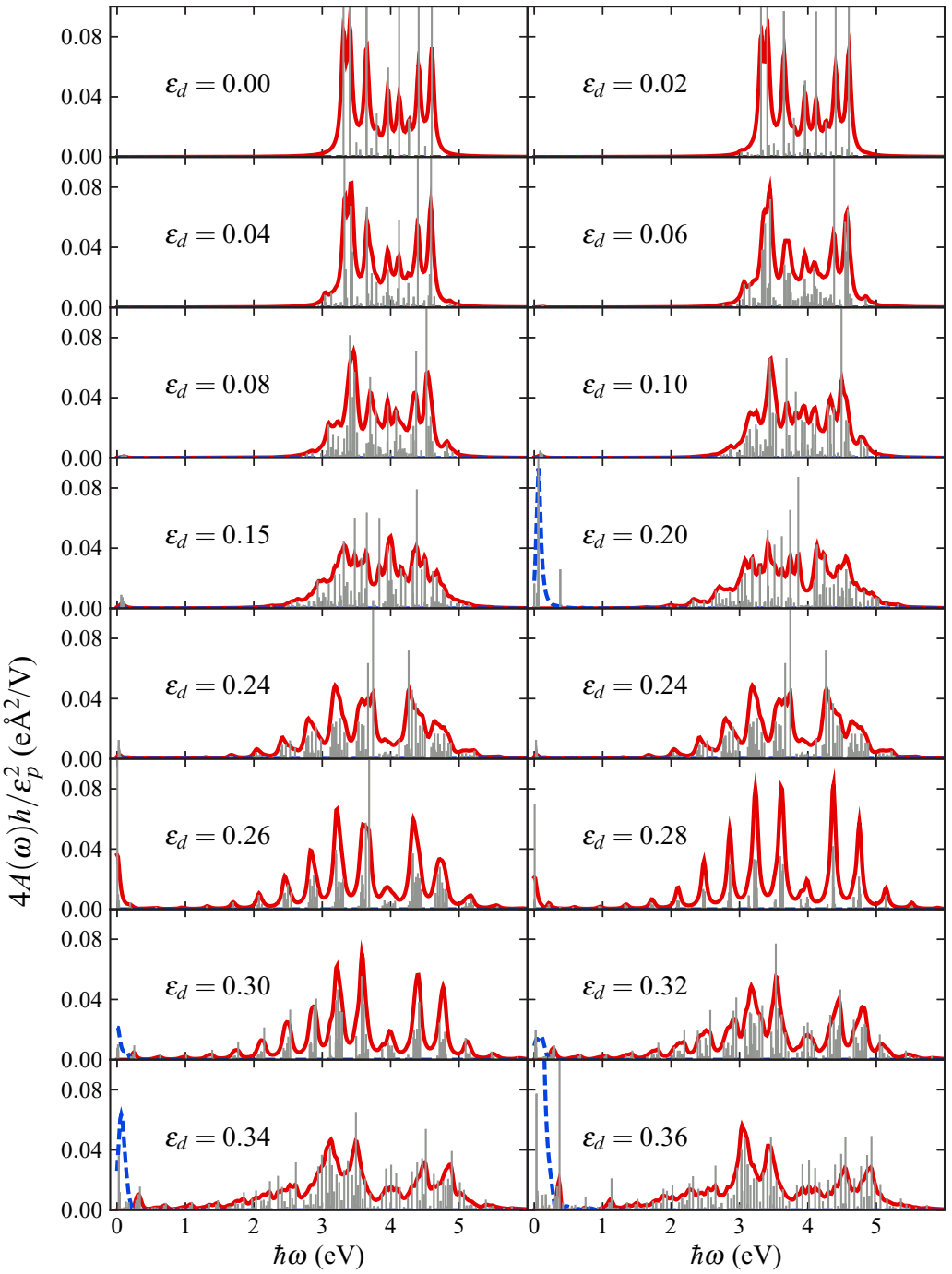

FIG. 3. Linear optical absorption spectrum for a semiconducting nanoparticle with Hamiltonian in Eq. (47) dressed with a continuous wave laser of varying amplitude ε_d (in V/Å). Red solid lines indicate net absorption, blue dashed ones indicate stimulated emission. The gray peaks signal the frequency and amplitude of each absorption transition between Floquet modes. Peaks are broadened by a Lorentzian function of width $\sigma = 0.04$ eV.

driving pulse is not generating any net charge carriers in the conduction band.

There are three essential features that emerge in the absorption as the electronic system is driven out of equilibrium: (i) *Below band-gap absorption.* As the driving amplitude increases in the 0–0.20 V/Å range we observe the emergence of additional spectral features just below the 3.2 eV band gap. This phenomenon has been experimentally observed before [39,40] and is reminiscent of the dynamic Franz-Keldysh effect [25] in solids and the quantum confined Stark effect in nanostructures [26]. (ii) *Broadband absorption.* A feature that is predicted by the theory is that by driving the nanoparticle nonresonantly it is possible to reversibly turn this IR-Visible transparent material into a broadband absorber. For instance, the nonequilibrium spectra for $\varepsilon_d = 0.24$–0.36 V/Å exhibits several absorption peaks across the IR-Visible region that

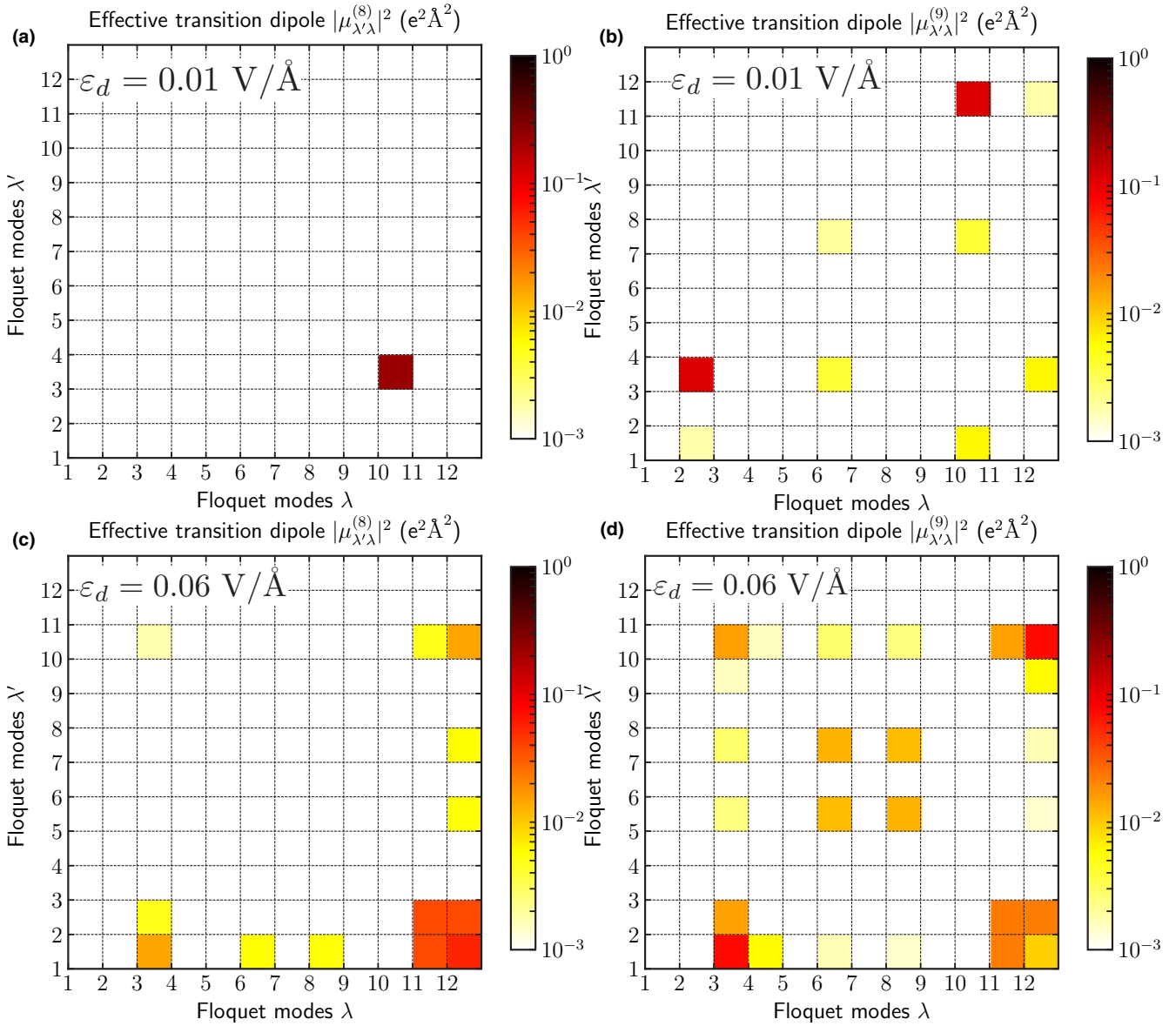

FIG. 4. Inter-FBZ transition dipoles $\mu^{(n)}_{\lambda',\lambda}$ between Floquet modes with indexes λ and λ' separated by n Brillouin zones. The figure contrasts results for weak $\varepsilon_d = 0.01$ V/Å (a), (b) and stronger $\varepsilon_d = 0.06$ V/Å (c), (d) driving field amplitudes. Note that all the nonvanishing elements of the transition dipoles for $n = 8$ have replicas in $n = 9$. They correspond to the transitions between the same Floquet modes but separated by different number of Floquet Brillouin zones.

are spaced by the photon energy of the driving light. (iii) *Low-frequency absorption and stimulated emission.* Another feature that emerges far from equilibrium are strong absorption and stimulated emission features in the THz region of the electromagnetic spectrum, as those exhibited for $\varepsilon_d = 0.20$ V/Å (emission) and $\varepsilon_d = 0.26$ V/Å (absorption). By driving the system out of equilibrium by nonresonant light, it is possible to completely change the absorption spectra of the driven materials in a reversible fashion and tune its optical properties. We now interpret these three basic features in the nonequilibrium absorption from a Floquet perspective.

1. Below band-gap absorption

As the driving field amplitude is increased up to 0.06 V/Å, the first thing that is observed is the emergence of an additional series of absorption peaks around 3.0–3.2 eV and a reduction of the intensity of the peaks around 3.3–3.4 eV. These peaks appear less than $\hbar\Omega$ away from the main absorption features at equilibrium and lead to a net red-shift in the absorption spectrum. This phenomenon can be understood in the context of Eq. (46) by examining the transition dipoles of the driven system. As shown in Fig. 4, as the driving field is increased from 0.01 V/Å [Figs. 4(a) and 4(b)] to 0.06 V/Å [Figs. 4(c) and 4(d)] there is an increase in the magnitude of the transition dipoles between Floquet modes that are $n = 8$ FBZs away that are responsible for these new spectral features. From Fig. 4 it is also clear that for $\varepsilon_d = 0.06$ V/Å, the nonvanishing elements of the transition dipole between Floquet modes separated by eight FBZs $\mu^{(8)}_{\lambda',\lambda}$ [Fig. 4(c)] have replicas in $\mu^{(9)}_{\lambda'\lambda}$ [Fig. 4(d)]. This indicates that

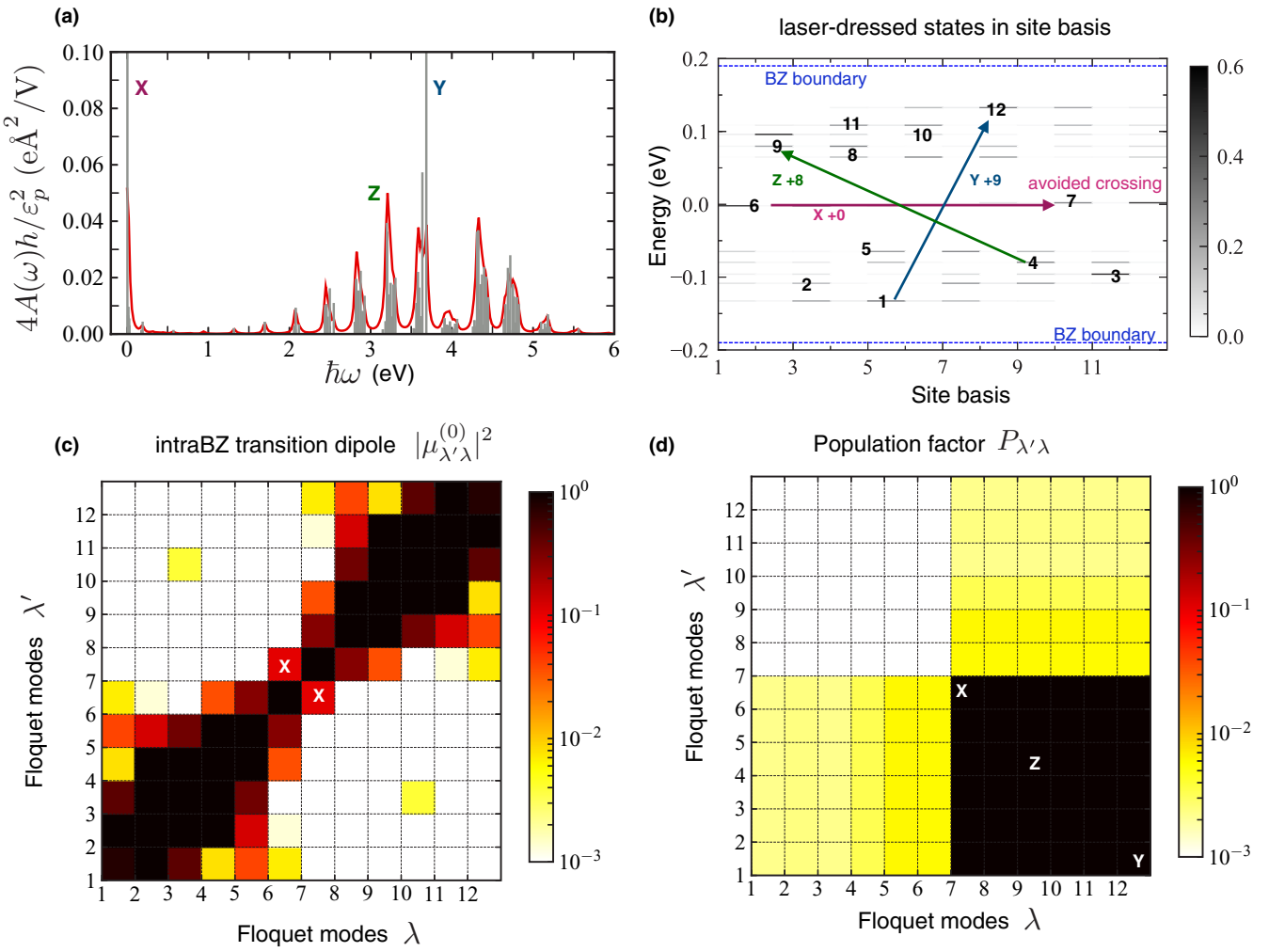

FIG. 5. Interpretation of the absorption spectrum for $\varepsilon_d = 0.26$ V/Å. The absorption spectrum (a) of the laser-driven material exhibits a strong absorption feature at low frequency (labeled X), and several absorption features in the IR-Visible-UV region that are periodically separated by $\hbar\Omega$ which make the material a broadband absorber. Two of them are labeled Y and Z. (b) Quasienergies of the Floquet modes in the first FBZ and population $|\langle k|\phi^0_\lambda\rangle|^2$ (gray scale) of the Floquet modes in the site basis at times $t_0 + nT$. The arrows signal optical transitions responsible for the X, Y, Z spectral features in (a), and the $+n$ the number of FBZs separating the two Floquet modes involved in the transition, e.g., X +0 means this is an intra-FBZ transition. (c) Effective dipole between Floquet modes within the first FBZ $|\mu^{(0)}_{\lambda\lambda'}|^2$. (d) Effective population factor $P_{\lambda\lambda'}$ ($\lambda' \to \lambda$) between Floquet modes. The numeric labels to the Floquet modes in (c) and (d) are those assigned in (b).

these spectral features can be understood as Floquet replicas of the transitions for *the nonequilibrium material*. By contrast when the system is close to equilibrium (i.e., for $\varepsilon_d = 0.01$ V/Å), $\mu^{(8)}_{\lambda',\lambda}$ and $\mu^{(9)}_{\lambda',\lambda}$ are completely different and just reflect the transition dipoles of the pristine material.

2. *Broadband absorption and spectral replicas*

As we increase the amplitude of the driving laser to $\varepsilon_d = 0.26$ V/Å (Fig. 3), the semiconducting material becomes a broadband absorber with the emergence of new absorption features in the IR-Visible region where the material was transparent and with a change in the spectral features in the UV region of the pristine material. Interestingly, the absorption spectra exhibit a clear periodic structure with spectral features separated by multiples of the driving photon energy $\hbar\Omega$.

To understand these features consider Fig. 5, which details the properties of the Floquet modes, population factors, and the intra-FBZ transition dipoles. The quasienergies and distribution of the Floquet modes along the chain are shown in Fig. 5(b). Floquet states 1–6 have quasienergies $0 > \mathcal{E}_\lambda > -\hbar\Omega/2$ and are composed mostly of Wannier states that form the valence band of the pristine material (of odd site states). In turn, Floquet states 7–12 have quasienergies $0 < \mathcal{E}_\lambda < \hbar\Omega/2$ and are composed mostly of Wannier states that form the conduction band. In this case, the population factors allow valence to conduction band transitions that originate in $\lambda' = 1$–6 and end in $\lambda = 7$–12. We observe that the Floquet modes are delocalized across the nanoparticle [Fig. 5(b)]. Interestingly, the degree of delocalization of the Floquet modes is smaller than the states of the pristine system, but larger than the Wannier-Stark states [41,42] that would have been obtained

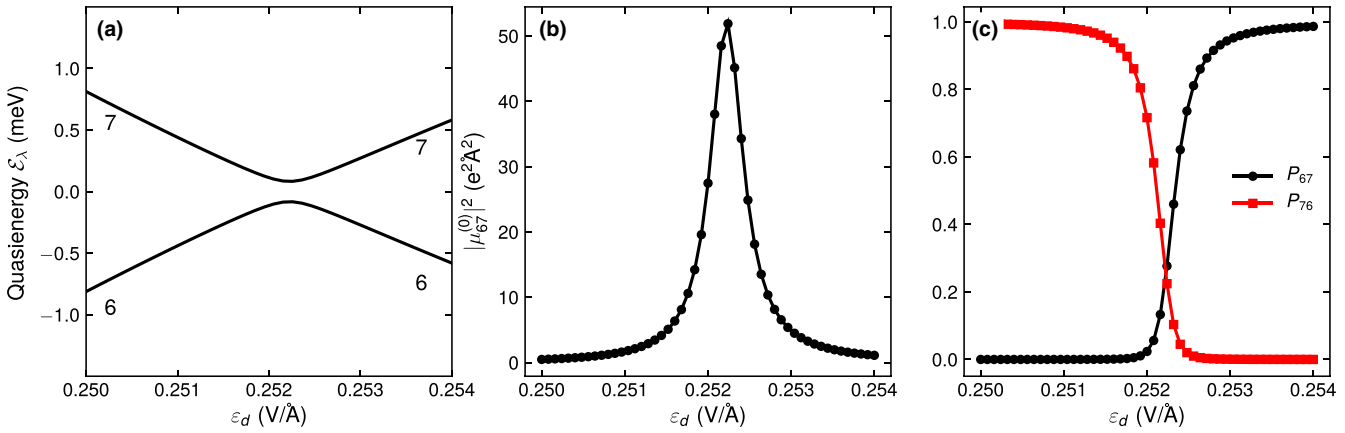

FIG. 6. (a) Quasienergy, (b) intra-FBZ transition dipole, and (c) population factors around the avoided crossing occurring at $\varepsilon_{d,\text{crossing}} = 0.2522$ V/Å in the first FBZ between Floquet modes 6 and 7. The hybridization of the two Floquet modes around the crossing leads to large intra-FBZ effective transition dipole $|\mu^{(0)}_{67}|^2$, population mixing between the two states, and absorption and stimulated emission features at meV frequencies.

by diagonalizing the Hamiltonian in the presence of a fixed electric field with amplitude 0.26 V/Å.

We label the largest absorption feature in the two main cluster of peaks around 3.2 and 3.6 eV in the absorption spectra [Fig. 5(a)] by Z and Y, respectively. As can be seen in Fig. 5(b), Y originates from transitions between Floquet modes $|\phi_1\rangle \rightarrow |\phi_{12}\rangle$ separated by $n = 9$ FBZs, while Z originates from $|\phi_4\rangle \rightarrow |\phi_9\rangle$ transition separated by $n = 8$ FBZs. Thus, the cluster of peaks separated by the driving photon energy originates from transitions that are separated by a different number of Floquet replicas. The absorption spectra have visible transitions between FBZs that are separated by $n = 3$–14 FBZs. Generally, the magnitude of the absorption decreases as the n FBZs that separate a given transition deviate from the $n = 8$–9 needed for a transition across the band gap in the near-equilibrium system. The contributions coming from lower n broaden the frequency regime for the absorption of the material, and turn it into a broadband absorber.

The periodic structure in the absorption spectra is a clear manifestation of the periodicity of the Floquet space. This remarkable feature is particularly evident for some special values of the driving electric field (see, e.g., 0.28 V/Å in Fig. 3). For such values, 10 of the 12 Floquet states cluster around 2 particular quasienergy values in the first FBZ, leading to a spectra with sharp periodic features. The remaining two Floquet states remain close to 0 and their relevance is discussed in Sec. III B 3. This spectral signature of the Floquet modes is complementary to those in photoemission spectroscopy [43].

3. *Low-frequency spectral features*

Surprisingly, for particular values of the driving electric field we observe a strong low-frequency (∼meV) absorption or stimulated emission band (see, for example, $\varepsilon_d = 0.20, 0.26, 0.36$ V/Å). These features can be probed using THz radiation or be used to generate THz pulses. The presence of net stimulated emission is a signature of the nonequilibrium nature of the Floquet states. In fact, the effective population factor $P_{\lambda\lambda'}$ [Eq. (45)] depends on the strength, frequency, and polarization of the driving light. To understand the underlying physics from a Floquet perspective, consider the transition that leads to this phenomenon for $\varepsilon_d = 0.26$ V/Å labeled as X in Fig. 5(a). As shown in Fig. 5(b), we identify the strongest low-frequency transition at $\hbar\omega = 4$ meV as the intra-FBZ transition from Floquet modes 6 to 7. These two states are both dipole and population allowed [see Figs. 5(c) and 5(d)].

As shown in Fig. 6(a), the Floquet modes 6 and 7 form an avoided crossing in the Floquet picture as the driving amplitude is changed around $\varepsilon_{d,\text{crossing}} = 0.2522$ V/Å. Away from the avoided crossing, these two states do not have a significant intra-FBZ transition dipole. However, as shown in Fig. 6(b), the hybridization of the two Floquet modes around the avoided crossing creates a strong transition dipole between the two levels that peaks at the crossing point $\varepsilon_{d,\text{crossing}}$. Such hybridization leads to very large absorption and stimulated emission features in the absorption spectra at low frequencies. In fact, as shown in Fig. 7, these low-frequency transitions are an order of magnitude stronger than even the largest absorption peak observed at equilibrium. The hybridization also opens a small energy gap that imposes a lower limit to the frequency of the transition that can be observed, in this case ∼0.2 meV.

Around the crossing, both absorption and stimulated emission are present. The dominant phenomenon depends on the population factor as the absolute value of the effective dipole is the same for both transitions (i.e., $|\mu^{(0)}_{\lambda'\lambda}| = |\mu^{(0)}_{\lambda\lambda'}|$). As shown in Fig. 7, stimulated emission dominates for driving electric fields $\varepsilon_d < \varepsilon_{d,\text{crossing}}$ because in this case $P_{76} > P_{67}$ [Fig. 6(c)], while absorption dominates for $\varepsilon_d > \varepsilon_{d,\text{crossing}}$ because $P_{67} > P_{76}$. For a driving electric field with amplitude right around the avoided crossing [Fig. 7(b)], a rich spectrum with both absorption and stimulated absorption features results. The additional peaks around $\hbar\omega = 0.38$ eV originate from transitions from Floquet modes 6 and 7 to equivalent states one FBZ away.

The avoided crossings in the Floquet picture are responsible for a number of phenomena such as bond softening and

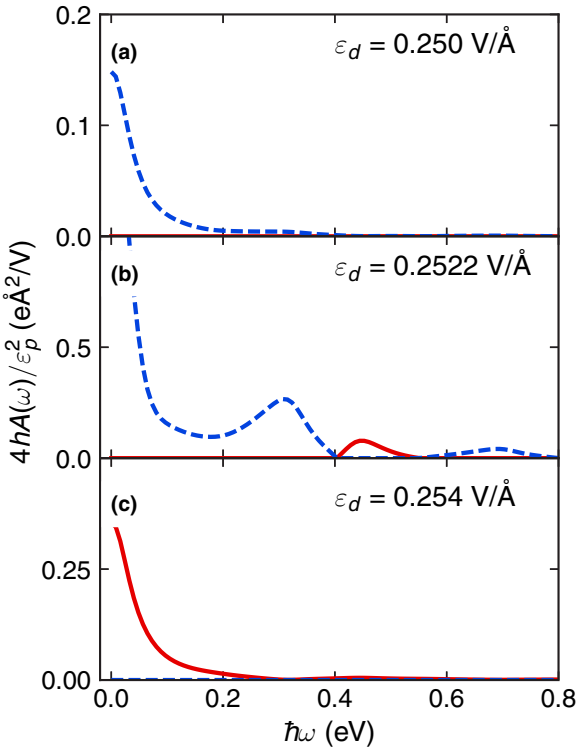

FIG. 7. Net absorption (red solid lines) and stimulated emission (blue dashed lines) spectra at low frequencies for a driving pulse (a) just below the avoided crossing shown in Fig. 6(a), (b) right at the crossing $\varepsilon_d = \varepsilon_{d,\text{crossing}}$, and (c) just above it. The low-frequency absorption spectra transition from stimulated emission to absorption as the driving electric field amplitude is increased across the avoided crossing.

hardening of diatomic molecules under intense laser driving [44,45] and coherent destruction of tunneling [46] under high-frequency driving. In this context, it leads to strong low-frequency absorption and emission due to hybridization of Floquet states.

IV. DISCUSSION

A. Summary of observations

In summary, we have developed a theory to study the optical absorption properties of laser-driven materials. The optical absorption in this nonequilibrium case is defined as the rate of transitions between laser-driven states due to interaction with the probe laser [Eq. (3)]. By treating the probe laser in first-order perturbation theory, it is possible to relate the nonequilibrium absorption spectra to the two-time dipole-dipole correlation function in the interaction picture of the laser-driven Hamiltonian [Eq. (14)]. To make further progress, we focused on effective noninteracting electronic systems for which the dynamics of the creation and annihilation operators in the driving pulse can be solved in closed form by invoking Floquet theorem [Eq. (32)]. In this way, we were able to treat the interaction between the driving electric field and matter exactly and reduce the complex time-dependent nonequilibrium calculations to a time-independent diagonalization in an extended Hilbert space.

These developments lead to a final expression [Eq. (46)] for nonequilibrium optical absorption which has a similar structure to the equilibrium one. In it, the Floquet modes play the role of system eigenstates and there are contributions due to absorption and stimulated emission. Transitions are allowed when a probe photon is at resonance with the transition frequency between two Floquet modes that have a nonzero transition dipole and that are allowed by populations. While the investigation of laser-matter interactions using Floquet approaches usually focuses on resonances between Floquet states [9,44,46], in this theory the focus is on the optical transitions induced by the probe light between Floquet modes. One unique feature of the nonequilibrium absorption theory is that the transition dipoles carry an additional index indicating the number of Brillouin zones separating the two Floquet modes.

To test the validity of the theory, we employed it to recover and interpret the well-known Autler-Townes effect. We further used the theory to characterize the nonequilibrium absorption of a model semiconducting nanoparticle reversibly driven far from equilibrium by nonresonant light. The computational analysis recovered the previously observed below band-gap absorption [39,40] and revealed two phenomena: (i) Nonresonant light turns this IR-Visible transparent material into a broadband absorber with multiple absorption features in the energy gap of the pristine material. These features are periodically spaced by the driving photon energy and are a characteristic signature of the periodic structure of Floquet space. They can be used as an optical signature of the presence of Floquet states. (ii) Nonresonant light opens strong low-frequency ($\sim$ meV) absorption and stimulated emission features at particular driving amplitudes. These features arise because of transitions between nearly degenerate Floquet modes that hybridize, thus enhancing their transition dipole. Such pair of states observe an avoided crossing with increasing driving electric field amplitude. Both low-frequency absorption or stimulated emission can be observed and tuned by changing the driving electric field amplitude around the avoided crossing. These three significant changes in the absorption properties of the model nanoparticle are present in a reversible regime of the laser-matter interaction where the driving pulse *per se* does not generate real carriers.

B. Qualitative picture of nonequilibrium absorption

At this point, it is useful to summarize these observations into a qualitative picture of the nonequilibrium optical absorption spectra. Figure 8 shows a schematic energy diagram of a semiconducting system in the presence of nonresonant driving light. In a Floquet sense, the dressing by the driving pulse leads to replicas of the valence and conduction band of the material that are separated by multiples of the driving pulse photon energy $n\hbar\Omega$. When the driving laser is weak, only optical transitions across the band gap E_g of the material are allowed. The levels involved are separated at least $m = \lfloor E_g/\hbar\Omega \rfloor$ FBZs away, where $\lfloor\cdot\rfloor$ denotes the floor function. For simplicity in presentation, let us suppose that E_g is precisely m FBZs away. Thus, the transition dipoles $\mu^{(n)}_{\lambda,\lambda'}$ for $n < m$ will be zero. As the amplitude of the driving laser field ε_d is increased, the replicas are distorted and previously forbidden inter-FBZ transition dipoles are created. The below

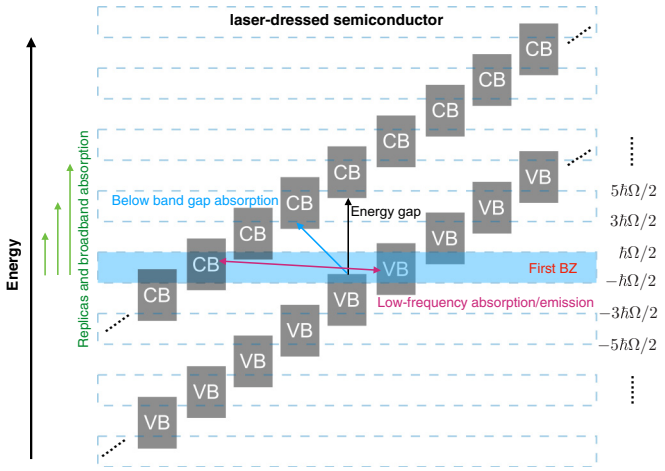

FIG. 8. Schematic of the energy diagram of a semiconductor dressed by nonresonant light of frequency Ω. The driving creates Floquet replicas of the valence (VB) and conduction (CB) band levels of the pristine material separated by integer $n\hbar\Omega$, leading to features in the absorption spectrum including below band-gap absorption, low-frequency transitions, and broadband absorption.

band-gap absorption occurs when those at $n = m - 1$ are allowed and these features are separated from E_g at most by $\hbar\Omega$. As ε_d is increased, additional absorption features are created for $n = m - 2, m - 3, m - 4, \ldots$ leading to periodic absorption features that are separated by multiples of $\hbar\Omega$ and that make this initially transparent semiconductor into a broadband absorber. Low-frequency ($\sim$ meV) optical features emerge when there are optically accessible intra-FBZ transitions or transitions between Floquet modes at adjacent FBZ edges, as schematically shown in the figure. For nonresonant driving, most of these transitions will be optically forbidden either through transition dipoles or population factors. Strong low-frequency transitions are opened when a pair of Floquet modes that are allowed by population factors enter into resonance and through hybridization create strong intra-FBZ transition dipoles.

C. Floquet prospects

Equation (46) indicates that the natural states to interpret the nonequilibrium absorption spectra are the Floquet modes and not the pristine states of the system. In terms of interpretation, this transition from pristine states to Floquet modes leads to a series of important changes in our intuition: (i) The transition dipoles between Floquet modes are time dependent, periodic in time, and admit a Fourier expansion [Eq. (34)] with component $\mu^{(n)}_{\lambda\lambda'}$ oscillating at frequency $n\Omega$. The $\mu^{(n)}_{\lambda\lambda'}$ component connects Floquet states that are n FBZs away, and determine which transitions open as the driving laser changes. This contrasts with the equilibrium case in which the transition dipoles between pristine eigenstates are time-independent quantities. (ii) Because the Floquet modes are time dependent, to develop intuition into which modes are dipole connected it is important to examine their spatial distribution at all times $t_0 < t \leqslant t_0 + T$ and not just at a particular time t_0. (iii) The population factors that determine which transitions are allowed depend on the initial state *and* the driving light. This contrasts with the equilibrium theory of absorption where this is just determined by the initial distribution of population among states. (iv) A natural subdivision of energy is the driving photon energy $\hbar\Omega$ that separates the different FBZs. As schematically shown in Fig. 8, one can interpret the optical properties by focusing on a given FBZ and examining inter-FBZ and intra-FBZ transitions. Except for high-frequency driving, the relevant Floquet transitions that signal interband absorption will not be for states in the same FBZ but for those separated $\lfloor E_g/\hbar\Omega \rfloor$ FBZs away.

The developed theory and interpretation is based on identifying optical transitions that are enabled in laser-driven matter. It applies for effective noninteracting electronic materials driven resonantly or nonresonantly by multichromatic light with commensurate frequencies of arbitrary strength. Such scheme can be used to design laser-driven materials with desirable nonequilibrium optical properties.

Future prospects include computations in realistic materials using *ab initio* based models, characterizing the role of electron-electron and electron-phonon interactions in the nonequilibrium absorption, and connecting the theory with other theories of absorption that have been developed for laser-driven matter [16,28,47–49].

ACKNOWLEDGMENT

This material is based upon work supported by the National Science Foundation under Grant No. CHE-1553939.

APPENDIX: NULLITY OF THE NEGLECTED TERM IN EQ. (43)

The neglected term in Eq. (43) is

$$I(\omega) = \frac{|\varepsilon_p|^2}{4\hbar^2} \lim_{t\to+\infty} \frac{1}{t - t_0} \iint_{-\infty}^{t} C_{\mu\mu}(\bar{t}, \tau)(e^{-i2\omega\bar{t}} + \text{c.c.})\, d\bar{t}\, d\tau, \tag{A1}$$

where

$$C_{\mu\mu}(\bar{t}, \tau) = \sum_{n,n'} \sum_{\lambda,\lambda',\eta,\eta'} \sum_{\gamma\delta\gamma'\delta'} D^{n}_{\lambda'\lambda\gamma\delta} D^{n'}_{\eta'\eta\gamma'\delta'} \times e^{i(\mathcal{E}_{\eta'\eta} + \mathcal{E}_{\lambda'\lambda})(\bar{t} - t_0)/\hbar + i(n'+n)\Omega\bar{t}} \times e^{i[(\mathcal{E}_{\eta'\eta} - \mathcal{E}_{\lambda'\lambda})/\hbar + (n'-n)\Omega]\tau/2} \langle c^{\dagger}_{\gamma} c_{\delta} c^{\dagger}_{\gamma'} c_{\delta'} \rangle .$$

To make an appreciable contribution, the argument in the exponent needs to vanish in order to cancel the factor $1/(t - t_0)$. Consider the $e^{-i2\omega\bar{t}}$ term in Eq. (A1) (the other term can be obtained simply by $\omega \leftrightarrow -\omega$). For the argument to vanish,

$$\mathcal{E}_{\eta'\eta} + \mathcal{E}_{\lambda'\lambda} = 0, \quad (n' + n)\Omega - 2\omega = 0. \tag{A2}$$

In turn, the integration with respect to τ yields the following delta function:

$$\delta((\mathcal{E}_{\eta'\eta} - \mathcal{E}_{\lambda'\lambda} + (n' - n)\hbar\Omega)/2). \tag{A3}$$

Inserting the first equality in Eq. (A2) into this delta function yields $\delta(\mathcal{E}_{\eta'\eta} - (n - n')\hbar\Omega/2)$. Thus, this term is nonzero when $\Omega = 2\mathcal{E}_{\eta'\eta}/\hbar(n - n')$. This condition, in general, is not satisfied except accidentally. Thus, the neglected term does not contribute to the final absorption spectrum.

[1] G. R. Fleming and M. A. Ratner, Phys. Today **61**(7), 28 (2008).
[2] W. Paul, Rev. Mod. Phys. **62**, 531 (1990).
[3] M. Grifoni and P. Hänggi, Phys. Rep. **304**, 229 (1998).
[4] S. Kohler, J. Lehmann, and P. Hänggi, Phys. Rep. **406**, 379 (2005).
[5] M. Rini, R. Tobey, N. Dean, J. Itatani, Y. Tomioka, Y. Tokura, R. W. Schoenlein, and A. Cavalleri, Nature (London) **449**, 72 (2007).
[6] D. Fausti, R. I. Tobey, N. Dean, S. Kaiser, A. Dienst, M. C. Hoffmann, S. Pyon, T. Takayama, H. Takagi, and A. Cavalleri, Science **331**, 189 (2011).
[7] M. Mitrano, A. Cantaluppi, D. Nicoletti, S. Kaiser, A. Perucchi, S. Lupi, P. Di Pietro, D. Pontiroli, M. Riccò, S. R. Clark, D. Jaksch, and A. Cavalleri, Nature (London) **530**, 461 (2016).
[8] B. R. Mollow, Phys. Rev. **188**, 1969 (1969).
[9] M. Fleischhauer, A. Imamoglu, and J. P. Marangos, Rev. Mod. Phys. **77**, 633 (2005).
[10] S. H. Autler and C. H. Townes, Phys. Rev. **100**, 703 (1955).
[11] E. I. Butikov, Am. J. Phys. **69**, 755 (2001).
[12] R. Kubo, J. Math. Phys. **4**, 174 (1963).
[13] M. S. Green, J. Chem. Phys. **22**, 398 (1954).
[14] R. Kubo, J. Phys. Soc. Jpn. **12**, 570 (1957).
[15] S. Mukamel, *Principles of Nonlinear Optical Spectroscopy* (Oxford University Press, Oxford, 1995).
[16] R. W. Boyd, *Nonlinear Optics* (Elsevier, Amsterdam, 2008).
[17] Y. Mizumoto and Y. Kayanuma, Phys. Rev. B **72**, 115203 (2005).
[18] Y. Mizumoto, Y. Kayanuma, A. Srivastava, J. Kono, and A. H. Chin, Phys. Rev. B **74**, 045216 (2006).
[19] M. Qasim, M. S. Wismer, M. Agarwal, and V. S. Yakovlev, arXiv:1804.09030.
[20] C. N. Cohen-Tannoudji, in *Amazing Light* (Springer, New York, 1996), pp. 109–123.
[21] I. Franco, M. Shapiro, and P. Brumer, Phys. Rev. Lett. **99**, 126802 (2007).
[22] L. Chen, Y. Zhang, G. Chen, and I. Franco, Nat. Commun. **9**, 2070 (2018).
[23] A. Schiffrin, T. Paasch-Colberg, N. Karpowicz, V. Apalkov, D. Gerster, S. Mühlbrandt, M. Korbman, J. Reichert, M. Schultze, S. Holzner, J. V. Barth, R. Kienberger, R. Ernstorfer, V. S. Yakovlev, M. I. Stockman, and F. Krausz, Nature (London) **493**, 70 (2013).
[24] M. Schultze, E. M. Bothschafter, A. Sommer, S. Holzner, W. Schweinberger, M. Fiess, M. Hofstetter, R. Kienberger, V. Apalkov, V. S. Yakovlev, M. I. Stockman, and F. Krausz, Nature (London) **493**, 75 (2012).
[25] L. V. Keldysh, ZhETF **34**, 1138 (1958) [Sov. Phys. JETP **7**, 788 (1958)].
[26] D. A. B. Miller, D. S. Chemla, T. C. Damen, A. C. Gossard, W. Wiegmann, T. H. Wood, and C. A. Burrus, Phys. Rev. Lett. **53**, 2173 (1984).
[27] R. Zwanzig, *Nonequilibrium Statistical Mechanics* (Oxford University Press, Oxford, 2001).
[28] E. Perfetto and G. Stefanucci, Phys. Rev. A **91**, 033416 (2015).
[29] G. Stefanucci and R. van Leeuwen, *Nonequilibrium Many-Body Theory of Quantum Systems: A Modern Introduction* (Cambridge University Press, Cambridge, 2013).
[30] A. Goussev, R. A. Jalabert, H. M. Pastawski, and D. Wisniacki, Scholarpedia **7**, 11687 (2012).
[31] E. Runge and E. K. U. Gross, Phys. Rev. Lett. **52**, 997 (1984).
[32] M. A. L. Marques, N. T. Maitra, F. M. S. Nogueira, E. K. U. Gross, and A. Rubio, *Fundamentals of Time-Dependent Density Functional Theory* (Springer, Berlin, 2012).
[33] S.-I. Chu and D. A. Telnov, Phys. Rep. **390**, 1 (2004).
[34] G. Floquet, Ann. Sci. Ec. Norm. Sup. **12**, 47 (1883).
[35] M. Combescot and R. Combescot, Phys. Rev. B **40**, 3788 (1989).
[36] X. Xu, B. Sun, P. R. Berman, D. G. Steel, A. S. Bracker, D. Gammon, and L. J. Sham, Science **317**, 929 (2007).
[37] R. Garcia-Fernandez, A. Ekers, J. Klavins, L. P. Yatsenko, N. N. Bezuglov, B. W. Shore, and K. Bergmann, Phys. Rev. A **71**, 023401 (2005).
[38] M. A. Sillanpää, J. Li, K. Cicak, F. Altomare, J. I. Park, R. W. Simmonds, G. S. Paraoanu, and P. J. Hakonen, Phys. Rev. Lett. **103**, 193601 (2009).
[39] S. Ghimire, A. D. DiChiara, E. Sistrunk, U. B. Szafruga, P. Agostini, L. F. DiMauro, and D. A. Reis, Phys. Rev. Lett. **107**, 167407 (2011).
[40] A. Srivastava, R. Srivastava, J. Wang, and J. Kono, Phys. Rev. Lett. **93**, 157401 (2004).
[41] G. H. Wannier, Phys. Rev. **117**, 432 (1960).
[42] M. Holthaus and D. W. Hone, Philos. Mag. B **74**, 105 (1996).
[43] Y. H. Wang, H. Steinberg, P. Jarillo-Herrero, and N. Gedik, Science **342**, 453 (2013).
[44] L. J. Frasinski, J. H. Posthumus, J. Plumridge, K. Codling, P. F. Taday, and A. J. Langley, Phys. Rev. Lett. **83**, 3625 (1999).
[45] B. Sheehy and L. F. DiMauro, Annu. Rev. Phys. Chem. **47**, 463 (1996).
[46] F. Grossmann, T. Dittrich, P. Jung, and P. Hänggi, Phys. Rev. Lett. **67**, 516 (1991).
[47] K. B. Nordstrom, K. Johnsen, S. J. Allen, A.-P. Jauho, B. Birnir, J. Kono, T. Noda, H. Akiyama, and H. Sakaki, Phys. Rev. Lett. **81**, 457 (1998).
[48] S. Pabst, A. Sytcheva, A. Moulet, A. Wirth, E. Goulielmakis, and R. Santra, Phys. Rev. A **86**, 063411 (2012).
[49] T. Otobe, Y. Shinohara, S. A. Sato, and K. Yabana, Phys. Rev. B **93**, 045124 (2016).